

A joint deconvolution algorithm to combine single dish and interferometer data for wideband multi-term imaging

Nikhil Vijay Naik*

August 5, 2017

Abstract

Imaging in Radio Astronomy is done by the means of either Single-Dish Radio Telescopes or Interferometric Array Radiotelescopes. Image Formation in a radio interferometer deals with calculating the inverse Fourier Transform of the Visibility Function $V(u, v)$. This strategy offers excellent angular resolutions but suffers from the *short-spacing* problem, where sources with large angular size and low surface brightness are not seen in an interferometer image. On the other hand, single-dish radio telescopes offer very coarse resolution, but respond very well to large angular scales.

This project aims to develop and prototype an algorithm to combine simulated data from these two types of telescopes, in order to bring about a good reconstruction of the true sky image at a wide range of frequencies. Consequently, an important physical parameter, *viz.* the spectrum of every source in the Field of View (FOV) is estimated from the reconstructed image.

*Indian Institute of Technology, Kharagpur, West Bengal, India - 721302

Contents

1	Introduction	3
1.1	Imaging with Single-Dish Radio Telescopes : Introduction	3
1.2	Imaging with Interferometric Arrays : Introduction	4
1.3	Motivation behind the Project and Problem Statement	5
2	Development of the Methodology and Algorithm	5
2.1	The Short Spacing Problem	5
2.2	Multi-Term, Multi-Frequency Wideband Imaging	6
2.3	Feathering	8
2.4	Putting everything together : Creation of the Algorithm	8
2.5	What this algorithm accomplishes	10
3	Testing the algorithm : Results and Plots	12
3.1	A Flat-Spectrum Sky	12
3.2	A Steep-Spectrum Sky	15
3.3	Comments and Discussion on the Results	17
4	Summary of the Project	18
5	Knowledge and Skills gained during this Project	18
5.1	New concepts learned during the project	18
5.2	Programming skills gained during this project	19
5.3	Practical Field Training	19
6	Acknowledgements	19
7	References and Bibliography	19
8	Appendix	20
8.1	Further extension of this work	20
8.2	Location of the Source Code and Data Use	22

1 Introduction

Radio Telescopes are used for creating images of the sky in the Radio Frequency regime of the Electromagnetic (EM) spectrum, which ranges from 3kHz to 300GHz [1]. Radio Telescopes belong to two distinct categories :

1. Single-Dish Radio Telescopes and
2. Interferometric Arrays.

1.1 Imaging with Single-Dish Radio Telescopes : Introduction

Single-Dish radio telescopes, such as the Robert C. Byrd Green Bank Telescope (hereafter GBT) are designed to respond linearly to the intensity of the radiation received from a point in the sky. The strategy followed to create an image from such an instrument is as follows :

The antenna beam ¹ sweeps across the region of interest. The response of each point on the sky as the beam sweeps across it is summed and put into a pixel. This is carried out for the whole Field-of-View (FOV) till the region has been fully sampled. This strategy is known colloquially as "basket-weaving", and is illustrated in Figure 1. The white circles represent beam sampling.

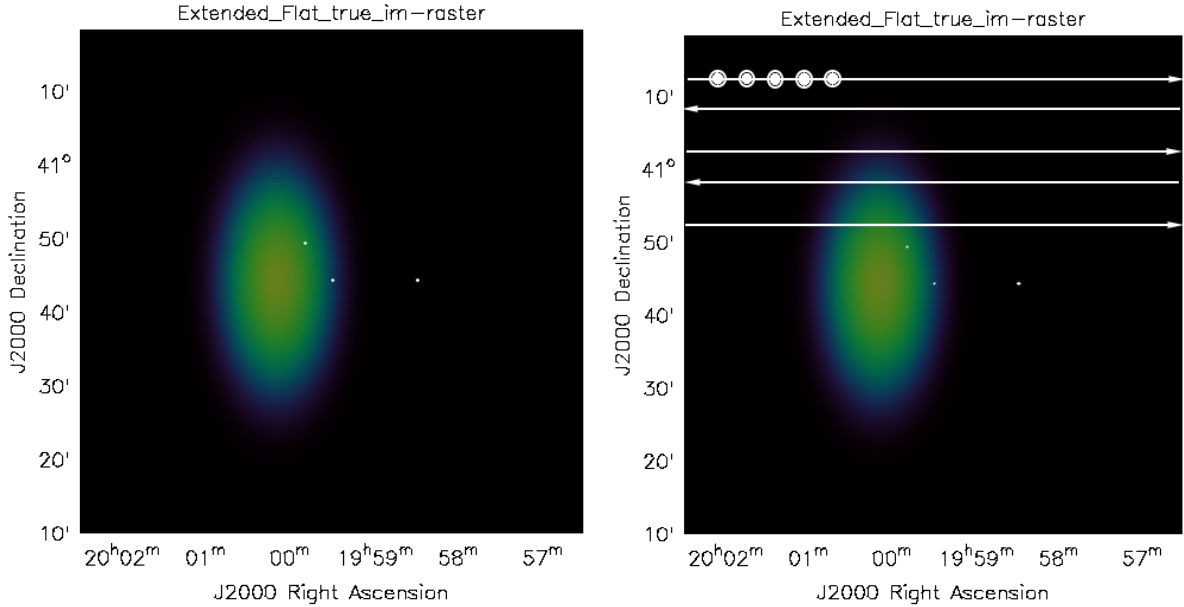


Figure 1: Illustration of the true sky image (left) and imaging using single-dish "basket weaving" technique (right)

Mathematically, the basket-weaving technique is equivalent to a *convolution*, where the antenna beam is *convolved* with the true sky image in order to form the image :

$$I^{Image} = I^{Sky} * P^{Antenna} \quad (1)$$

where $P^{Antenna}$ is the beam or hereafter the *Antenna Power Pattern*, and '*' denotes the convolution operator.

Properties of Single-dish images From the theory of diffraction, it is known [2][3] that the highest possible resolution in an image that is created from an aperture of diameter D for radiation of wavelength λ is given by

$$\theta \sim \frac{\lambda}{D} \quad (2)$$

From this equation, it is immediately seen that the resolution for radio frequencies is rather coarse. For the GBT dish with a diameter of 100m, the resolution at $\nu \sim 1.5\text{GHz}$ is still ~ 5 arcmin. Hence, single dish radio-telescopes are not useful for obtaining high-resolution radio images. This logically leads to the technique of interferometry for conducting high-resolution imaging.

¹It is the spatial response of the antenna to a source of unit intensity located in the sky.

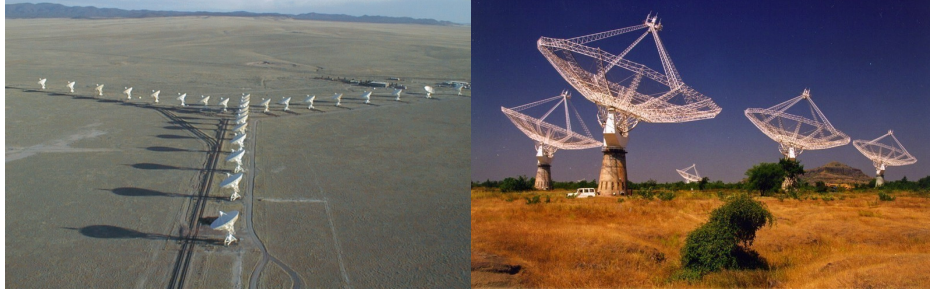


Figure 2: Examples of interferometers : The Very Large Array (VLA) (left) and the Giant Metrewave Radio Telescope (GMRT) (right). Image credits - NRAO and NCRA (VLA and GMRT respectively)

1.2 Imaging with Interferometric Arrays : Introduction

Interferometric arrays (Figure 2) are telescopes that have multiple elements or antennas. The radiation received at each antenna is combined using signal-processing software/hardware for creating the image - this technique is called 'Interferometry'. Each pair of antennas measures an *interference fringe*, and n antennas give $\frac{n(n-1)}{2}$ such fringes. Measurement of these fringes leads to the mathematical reconstruction of the *Visibility Function* $V(u,v)$. By the Van Cittert - Zernicke theorem of optics, it is known that the Intensity of radiation in the plane² of the sky and the visibility function are related by a two-dimensional Fourier transform [2][3][4][5]. Mathematically, we write

$$V(u,v) = \iint \frac{I(l,m)}{\sqrt{1-l^2-m^2}} e^{-2\pi i[lu+mv]} dudv \quad (3)$$

Where $V(u,v)$ is the visibility function, $I(l,m)$ is the intensity in space, l,m are the *direction cosines* and (u,v) are the *Fourier-domain* coordinates. A deeper treatment of interferometry, along with its mathematics can be found in [2][3][4].

Properties of interferometer images From Equation (2), we know that the finest resolution that can be measured by an aperture of diameter D is λ/D . In case of an interferometer, D is the *longest baseline*, defined as the maximum separation between a pair of antennas, which is unconstrained. This makes the technique of interferometry extremely powerful and it leads to very high-resolution images (arcsecond or sub-arcsecond) of the radio sky. As can be seen in Figure 3, the image of the same sky as seen by a single-dish radio telescope and an interferometer can look very different in terms of resolution.

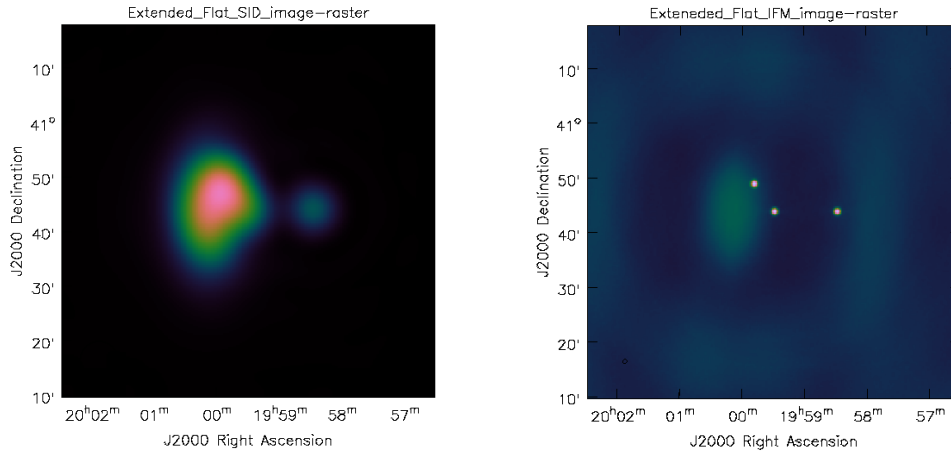


Figure 3: Image of the true sky from Figure 1, reconstructed using a single dish telescope (left) and an interferometer (right).

²If the FOV is too large, the assumption of the sky being a plane does break down

Note the point sources are almost completely absent on the left, but the extended source in the interferometer image on the right is imaged very faintly. This observation forms an important justification for this project.

1.3 Motivation behind the Project and Problem Statement

As was seen in Figure 3, a single-dish instrument provides images with very coarse resolution. An interferometer provides images with excellent resolution, however, it does not faithfully reproduce objects that have very large angular sizes and low surface brightness. Scientific goals of various kinds can be achieved by combining best of what these two classes of instruments have to offer.

Techniques such as *feathering*[6] exist to combine the two kinds of images. However, these suffer from many problems, rendering them insufficient as a reliable technique for image combination. These include :

1. It depends heavily on the arbitrary scaling of single-dish data, which may not always lead to physically sensible results.
2. It works only for data taken at exactly one frequency. It fails to utilise the vast potential of multi-frequency data taken with modern telescopes such as the VLA or the GMRT.
3. Wideband Imaging algorithms exist (Rau and Cornwell 2011)(Rau 2011, PhD thesis) for pure interferometer data, but due to the inherent limitations of imaging with an interferometer (called the *short spacing problem*), these are not useful for sources which have large angular extent.

This project aims to resolve all these deficiencies associated with feathering and wideband image reconstruction, namely, the dependency on the single-dish scaling and the short-spacing problem.

Problem Statement : Development of a joint deconvolution algorithm to combine single dish and interferometer data for wideband multi-term imaging.

2 Development of the Methodology and Algorithm

This section breaks down the problem statement into its component sub-problems. In Section 2.4, the individual solutions are put together to develop the final algorithm which is heuristically described.

2.1 The Short Spacing Problem

By the Van Cittert-Zernicke theorem (Section 1.2 and references therein), the Fourier Transform of the intensity (as a function of space) is the *complex visibility function*. Hence, the Fourier transform of the reconstructed image will give the sampled visibility function (in the discrete case).

The short spacing problem is illustrated in Figure 4. As can be seen, the Fourier transform of the interferometer image insufficiently samples the region around (0,0). This is called the *central uv-hole*. On the other hand, the single-dish data samples this precise region very well (Figure 4 bottom half), but lacks the data at large values of (u,v). This is overcome using the feathering technique, but it suffers from a few problems. The technique and its shortcomings are discussed in Section 2.3. The origin of the short spacing problem is briefly described below.

The (u, v) coordinate system is defined as follows [2][3](Rau and Cornwell 2011)(Rau 2011, PhD thesis):

$$u = \frac{b_{E-W}}{\lambda} \qquad v = \frac{b_{N-S}}{\lambda}$$

Where, b_{E-W} and b_{N-S} are the lengths of the baselines (*i.e.* - the separation between two antennas) in the East-West and North-South direction respectively. As any two antennas must always be separated by a finite nonzero distance, the values u and v can never be simultaneously zero. Hence, the smallest spacings always remain unsampled.

As sources with large angular extent have visibility values clustered around the origin, they are always undersampled and missed by the interferometer. This is clearly seen in Figure 4³. The interferometer (VLA) samples large values of the (u,v) plane but leaves out the area near (0,0). On the other hand, the Single-dish telescope (GBT) does not sample large values of (u,v) but densely samples the centre

³Note that the image in Figure 4 is flipped.

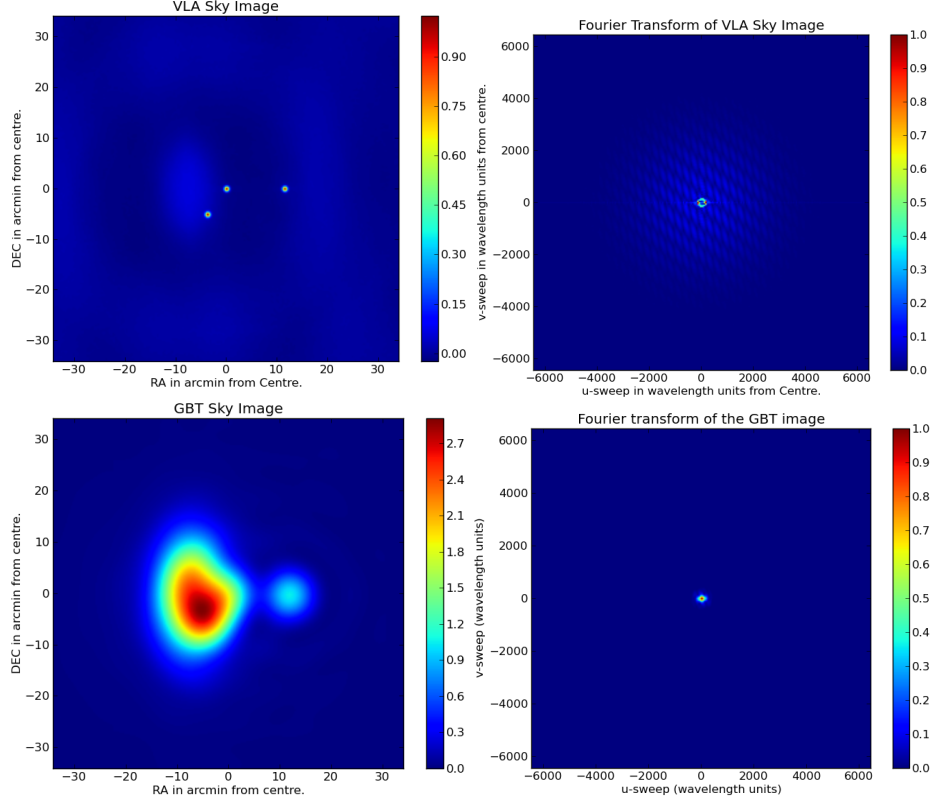


Figure 4: The short spacing-problem.

2.2 Multi-Term, Multi-Frequency Wideband Imaging

The description of a narrow-band multiterm multifrequency algorithm draws heavily from two sources : Rau and Cornwell 2011 and "Parameterized Deconvolution For Wide-Band Radio Synthesis Imaging" (Ph.D. dissertation of Urvashi Rau Venkata at the NRAO). Any radio image containing information on multiple angular scales can be written as a linear sum of a *sky model* comprising of δ functions, and a *smoothing kernel* which is usually a tapered, inverted, truncated paraboloid (Cornwell 2008). Mathematically, this amounts to

$$\mathbf{I}^m = \sum_{s=0}^{N_s-1} \mathbf{I}_s^{shp} * \mathbf{I}_s^{sky,\delta} \quad (4)$$

\mathbf{I}^m is the model sky image, \mathbf{I}_s^{shp} is the kernel function and $\mathbf{I}_s^{sky,\delta}$ is the δ function model of the sky. '*' denotes the convolution operator. The sky changes with the observing frequency. To model this frequency dependence, the sky is modeled as a Taylor series about a centre frequency :

$$\mathbf{I}_\nu^m = \sum_{t=0}^{N_t-1} w_\nu^t \mathbf{I}_t^{sky} \quad (5)$$

Moreover, the dependence of the sky on the frequency is modeled as a power-law with a curvature term :

$$\mathbf{I}_\nu^{sky} = \mathbf{I}_{\nu_0}^{sky} \left(\frac{\nu}{\nu_0} \right)^{I_\alpha^{sky} + I_\beta^{sky} \log(\frac{\nu}{\nu_0})} \quad (6)$$

Next, putting together equations (4) and (5) leads to :

$$\mathbf{I}_\nu^m = \sum_{s=0}^{N_s} \sum_{t=0}^{N_t} w_\nu^t [\mathbf{I}_s^{shp} * \mathbf{I}_{s_t}^{sky}] \quad (7)$$

In all these equations, $w_t = \left(\frac{\nu - \nu_0}{\nu_0} \right)^t$

In Equation (7), \mathbf{I}_s represents a collection of δ -functions that describe the sky locations and amplitudes of flux

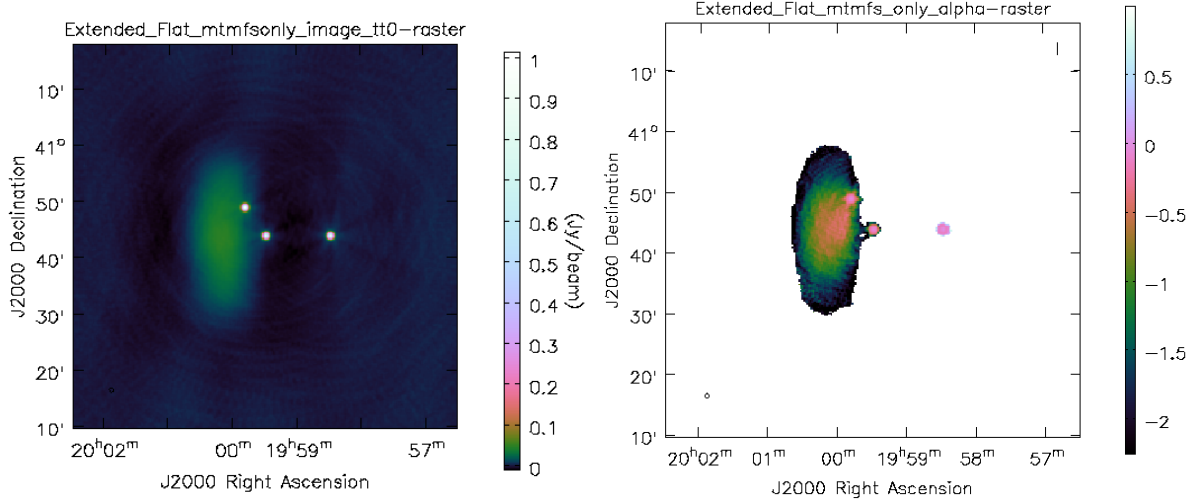


Figure 5: The reconstructed multiterm images using pure MTMFS for the sky shown in Figure 1

components corresponding to angular scale s in the image formed by the t^{th} Taylor series coefficient. (Rau and Cornwell 2011, section 2.2).

Using the convention outlined in Appendix A of Rau and Cornwell 2011, the relation between the image \mathbf{I} , the visibilities \mathbf{V} can be expressed in Matrix notation as:

$$\mathbf{V}_{n \times 1}^{obs} = [\mathbf{S}_{n \times m}] [\mathbf{F}_{m \times m}] \mathbf{I}_{m \times 1}^{sky} \quad (8)$$

where $\mathbf{V}_{n \times 1}^{obs}$ is the vector containing the observed visibilities, $[\mathbf{S}_{n \times m}]$ is the matrix that indicates sampling on the (u, v) plane, $[\mathbf{F}_{m \times m}]$ is the Fourier Transform operator and $\mathbf{I}_{m \times 1}^{sky}$ is the pixelated image of the sky intensity. Using this convention, the equation relating visibilities to the sky intensity at a given frequency ν becomes :

$$\mathbf{V}_{\nu}^{obs} = \sum_{s=0}^{N_s} \sum_{t=0}^{N_t} w_{\nu}^t [\mathbf{S}_{\nu}] [\mathbf{T}_s] [\mathbf{F}] \mathbf{I}_{s_t}^{sky} \quad (9)$$

In this case, $[\mathbf{T}_s]$ is a frequency *taper function*. Further description of this function can be found in Rau and Cornwell 2011. For multiple frequencies to be imaged in the same data set, we can stack the frequency weights in the matrix $[\mathbf{S}_{\nu}]$. The weight function w_{ν} will also become a matrix in this case, $[\mathbf{W}_t^{mfs}]$. Rewriting equation (9) in this form, one obtains :

$$\mathbf{V}^{obs} = \sum_{s=0}^{N_s} \sum_{t=0}^{N_t} [\mathbf{W}_t^{mfs}] [\mathbf{S}] [\mathbf{T}_s] [\mathbf{F}] \mathbf{I}_{s_t}^{sky} \quad (10)$$

Here, \mathbf{V}^{obs} is now an $nN_c \times 1$ matrix of *multi-frequency* visibilities, $[\mathbf{S}]$ is the (u, v) sampling function of the multi-frequency data.

Comment on the structure of the matrix $[\mathbf{W}_t^{mfs}]$ $[\mathbf{W}_t^{mfs}]$ is diagonal $nN_c \times nN_c$ matrix of weights. It consists of N_c diagonal blocks of size $n \times n$, and contains w_{ν}^t in its blocks.

Multiterm, Multi Frequency Synthesis Image formation The interferometer data records visibilities from various frequencies. The MTMFS imaging algorithm plots all these visibilities on a single (u, v) grid and recreates the dirty image set \mathbf{I}_t^{sky} through the matrix inversion route. This dirty images will then be fed to the MTMFS deconvolver which deconvolves the dirty images using a set of pre-defined angular scales [9]. The output will be a set of Taylor images that will encapsulate the multiterm data.

Limitations of the MTMFS deconvolution algorithm The MTMFS algorithm detailed in Rau and Cornwell 2011 uses only pure interferometer data. Due to the short-spacing problem (Section 2.1), it does not work for sources that have low surface brightness and large angular extents. However, there are important science goals

that can be achieved by extending to this technique for such sources. This can be clearly seen in Figure 5, where the zeroth-order Taylor image looks almost identical to that of Figure 8, but the spectrum is not reproduced properly at any point on the extended clous source.

2.3 Feathering

Feathering is the technique that is conventionally used to combine images from single-dish instruments and interferometers. A brief description of the feathering technique is presented below.

The composite image formed by feathering two images is obtained by computing a weighted sum in the Fourier domain and inverting the modified data to create the image. The weight given to the interferometer image is $(1 - \mathcal{F}(P_{antenna}))$, where \mathcal{F} is the Fourier transform and $P_{antenna}$ is the antenna pattern defined in (Section 1.1). The Fourier transform of the single-dish image is multiplied by the volume ratio of the interferometer *restoring beam* to the single dish antenna pattern [6]. Mathematically, this amounts to :

$$\mathcal{F}(\mathbf{I}^{feathered}) = \frac{w_s V_s + w_I V_I}{w_s + w_I} \quad (11)$$

here, V_s and V_I are the Fourier transforms of the single-dish and interferometer data respectively. Generally, the single-dish data is also pre-scaled by a gain parameter.

Limitations of the feathering algorithm The feathering algorithm suffers from a few limitations, including:

1. It depends strongly on the single-dish gain parameter which is used to pre-scale the single-dish data before beginning the calculation. This may lead to situations where the data is scaled too much and does not reflect the physical reality.
2. It does not allow manipulation of the visibility data from the raw data file, as it takes the final images as its input which have already been deconvolved and processed. Hence one cannot handle any potential artifacts which may crop up.
3. It is highly sensitive to noise levels in the data.

2.4 Putting everything together : Creation of the Algorithm

To overcome the problems detailed in Section 2.2 and Section 2.3, a new algorithm is needed which is developed in this project. The implementation of the algorithm uses tools from the `scipy`⁴, `numpy`⁵ and `CASA`⁶ software packages. All the programming was done in the `python` programming language, and all plots were created using either the `CASAvier` tool or the `matplotlib` plotting package.

Conventional (Cube) Radio Imaging from Interferometer Data

For data from a pure interferometer, the algorithm followed for imaging is as follows [10]:

Setup of the imaging procedure

1. The *uv cell size* in the image is decided. The size of a *uv* - cell is decided by the width of the *point spread function*⁷, which is the inverse Fourier transform of the *uv* - sampling function **[S]** (Section 2.2). Usually the cell size is chosen so that the main lobe of the PSF is Nyquist-sampled.
2. The visibility data is irregularly sampled - Hence, we need to first *regrid* the image along a regular grid so that the Fast Fourier Transform (FFT) algorithm will work.
3. Some visibility points are sampled more than others - hence, *weight* these visibilities appropriately to ensure that information from all the points is included in the image.

⁴<https://scipy.org/>

⁵<https://www.numpy.org>

⁶CASA stands for Common Astronomy Software Application. Webpage : https://casaguides.nrao.edu/index.php/Main_Page

⁷hereafter PSF

Joint Imaging and Deconvolution Procedure

- **Major Cycle :**

1. The raw data is regridded and weighted appropriately.
2. The weighted, gridded data is inverse Fourier transformed to form the *dirty image*.

- **Minor Cycle :**

1. The *dirty image* is passed to a *reconstruction* algorithm such as Hogböm CLEAN/MTMFS [2][3](Rau 2011, PhD thesis)[10].
2. After a number of iterations, the algorithm checks for convergence as specified in the input of the program. If the number of iterations has been reached, the cleaned image is written out.

- **After the Minor Cycle**

1. The cleaned image (the *model image*) is Fourier-transformed back onto the (u, v) plane.
2. This (u, v) plot is *degridded* and saved as a *model* visibility data, which is subtracted from the original visibility file.
3. The program then *loops back to the major cycle* using this modified visibility data. The model is updated by adding the output from each execution of the minor cycle. This looping is continued till the desired threshold limit is reached.

The algorithm developed in this project differs in a few major ways from the strategy outlined above due to the following reasons :

1. Feathering does not accept multi-frequency data gridded on to the same plane, because the antenna power pattern changes with frequency. Hence, it is necessary to compute the Taylor series of Equation (5) at all the values of the frequencies present in the data, and include a header containing the antenna beam or power pattern information has to be supplied to the feathering routine, implemented in **CASA** as the **feather()** task.
2. The subtraction of the model visibilities from the available data set in the Major cycle needs separate data and not the multi-frequency one. Hence, the MTMFS deconvolver has to be accordingly modified to output the multiple model images at multiple frequencies.
3. The MTMFS imager needs multiple PSFs as part of the deconvolution process. These need to be calculated during the run of the imager setup.

Conceptual differences between the narrow-band MTMFS algorithm and the new Wideband Multiterm Combination Algorithm

1. The Multiterm Wideband Combination Algorithm developed in this project does a joint deconvolution, namely, that it feathers both the single-dish data as well as the PSF with the corresponding interferometer ones. In case of a single-dish telescope, the PSF is simply the antenna beam or the power pattern.
2. In the first run of the setup, the gridded interferometer residual is first feathered with the single-dish data, then passed on to carry out the deconvolution.
3. After the run of each minor cycle, the multiterm images are converted back to the images at all the observing frequencies as a model (hereafter called a "cube" of images) .Thereafter, the residual contribution of the single dish image is calculated by smoothing these "model" images with their respective beams at their respective frequencies.
4. After the run of each major cycle, the single-dish residual images are recalculated. These are then again feathered with the interferometer residuals and written out.
5. These composite residual images are converted back into the multiterm residuals and the cycle is begun afresh.

A detailed description of the algorithm is presented as follows :

- The setup is broken into two parts: The setup for the 'Cube' image and the setup for the 'Multiterm' image.

- The 'Cube' setup is run first - This creates the initial cube PSFs and the initial cube of residual images.
- The 'MTMFS' setup is run - This creates the multiterm PSFs and the initial multiterm residuals.
- **Initial Setup consists of the following steps:**
 1. The PSFs from the interferometer and the single-dish image are feathered together, followed by the feathering of the single dish and interferometer residual. All the images in this step are the ones generated as 'cube' images.
 2. The multiterm PSFs are then calculated from the Cube PSFs, and written out to the appropriate number of files.
 3. The multiterm residuals are then calculated in the same way as the PSFs and are written out to the appropriate number of files.
- *The imaging and deconvolution part:*
While the imager has not converged:
 1. Run the multiterm Minor cycle using the PSFs calculated in the initial setup and the residual from the previous iteration. For the first iteration, use the residual calculated in the initial setup.
 2. Once the multiterm minor cycle is done, convert the multiterm model to a cube model and write it out to a file.
 3. With this model, run the next (Cube) Major cycle.
 4. Calculate the single-dish residual using the smoothed model output above and feather it with the interferometer residual cube.
 5. Convert this feathered cube residual into its multiterm equivalent and proceed to the next iteration.

Salient features of this algorithm

1. Note that, the minor cycle employs the multiterm deconvolution strategy whereas the major cycle uses a cube Gridding/FFT path.
2. Note that, while feathering, all the residuals are always in cube form.
3. Note that, all the cube data which were used during feathering has to be converted back into its multiterm form before being passed to the minor cycle.

2.5 What this algorithm accomplishes

A run of this algorithm produces the following outputs :

- A number of images equal to the number of terms in the Taylor series is produced.
- Residual images and model images equaling the number of terms in the Taylor series are produced by the multiterm algorithm, plus a cube residual and model produced by the cube portion of the major cycle.
- A spectral index map is produced by the multiterm portion of the algorithm, which shows the spectral index of the sky for each pixel in the image. Another image that holds the errors for the index estimates per pixel is also created.
- For n terms, this algorithm creates $2n - 1$ multiterm PSFs and one cube PSF.

Significance of each output

1. The images produced as output by this algorithm are the intensities \mathbf{I}_t^{sky} in Equation(5).
2. The residual images are equivalent to the iterations of the Fourier transform of the visibility matrix \mathbf{V}^{obs} in Equation (10).
3. The spectral index map is the solution of Equation (6). The maps are basically the pixel-wise estimate of the terms \mathbf{I}_α and \mathbf{I}_β .
4. The spectral PSFs are the inverse Fourier transform of the sampling matrix $[\mathbf{S}]$.

For the sky shown in Figure 1, the output images are shown in Figure 6 (Larger images are presented in the Results section).

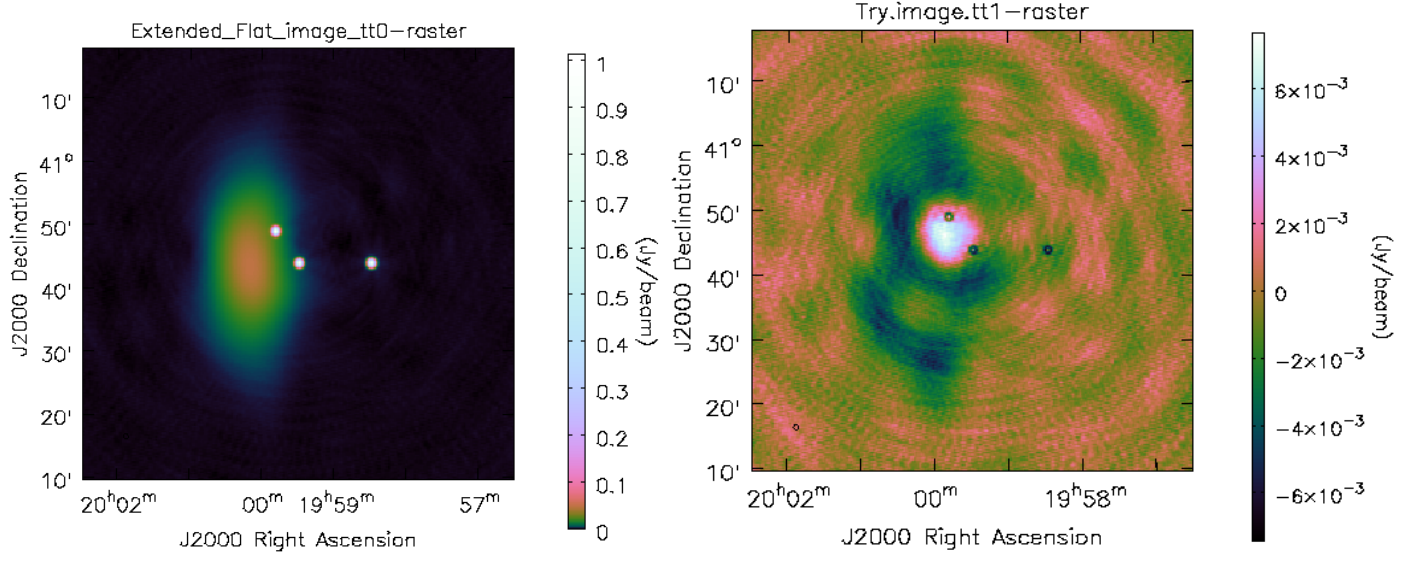


Figure 6: The reconstructed multiterm images for the sky shown in Figure 1

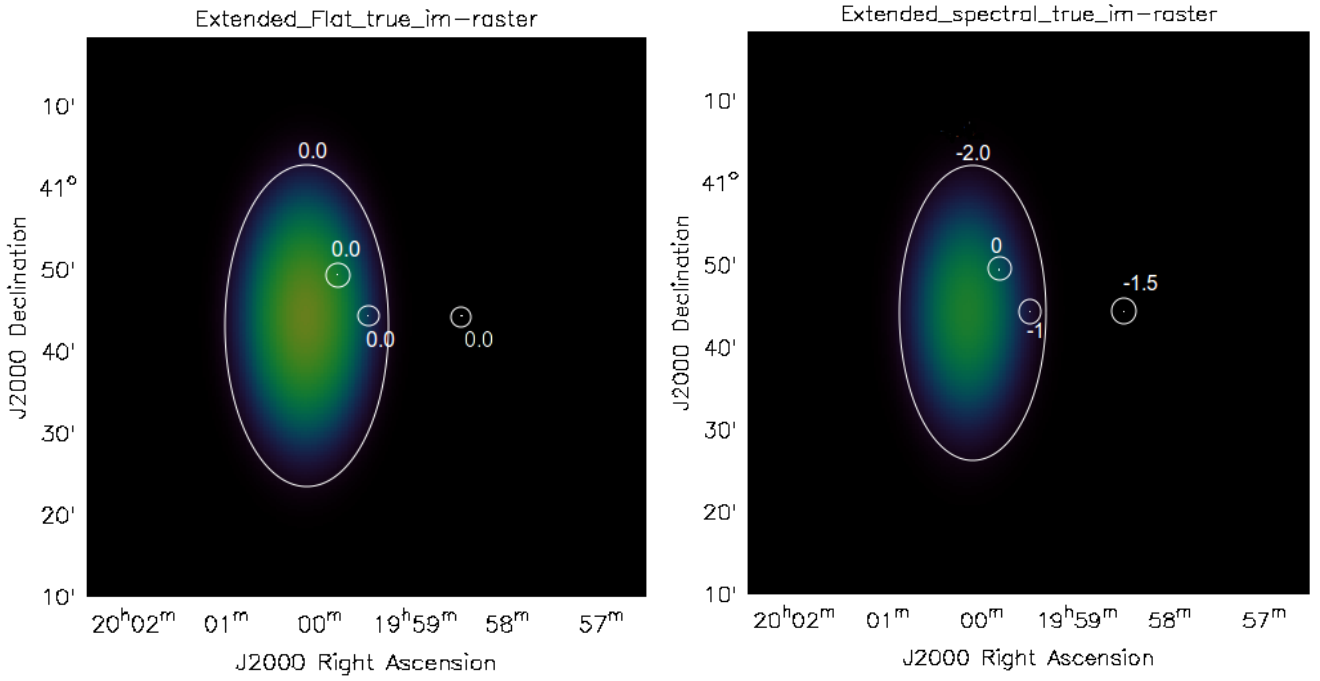


Figure 7: Two different simulated "sky images" with different spectral indices

3 Testing the algorithm : Results and Plots

This new algorithm was tested on two different test cases, both of which derive from Figure 1 :

1. A *flat-spectrum* sky, where the sky does not change with frequency. In this case, the plot of the spectrum must show a value of zero for every pixel
2. A *steep-spectrum* sky, where each object shown in Figure 1 has a nonzero spectral index. The spectral indices are indicated on the true sky image.

Both these "true skies" are shown in Figure 7.

3.1 A Flat-Spectrum Sky

Here, the reconstructed images from the Flat-spectrum sky are shown (true sky image shown in Figure 7-left panel)

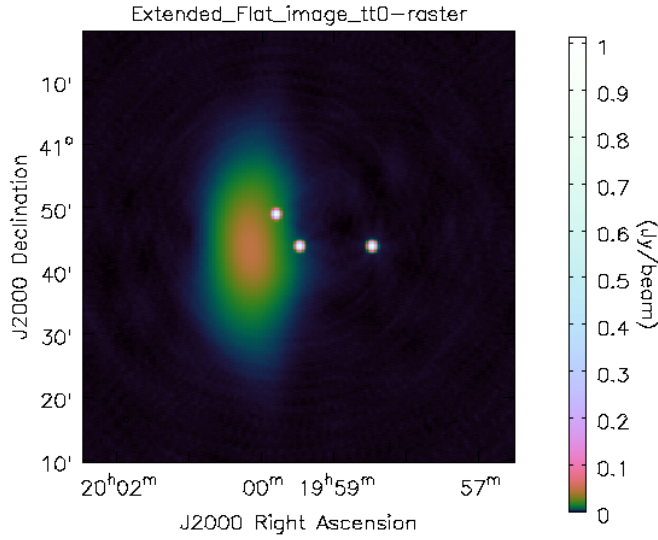


Figure 8: The zero-order Image of the Flat-spectrum sky

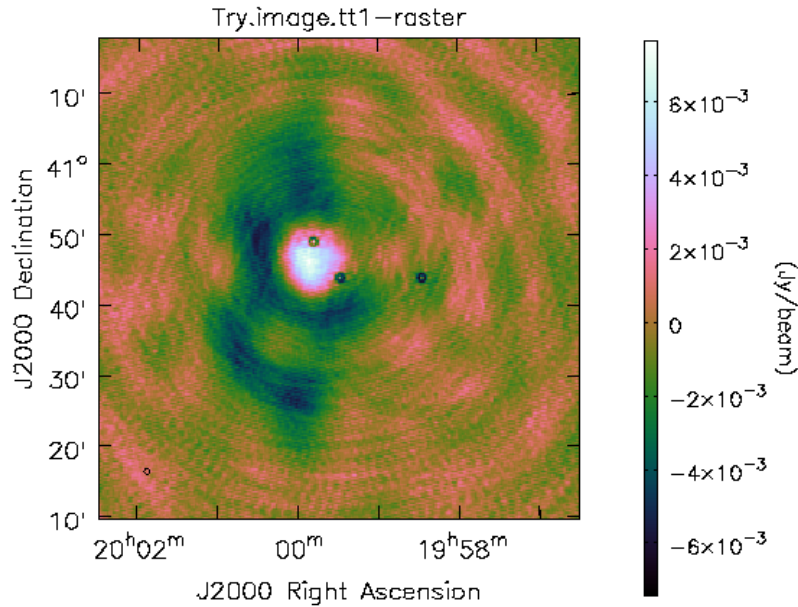


Figure 9: The 1st order Image of the flat-spectrum sky

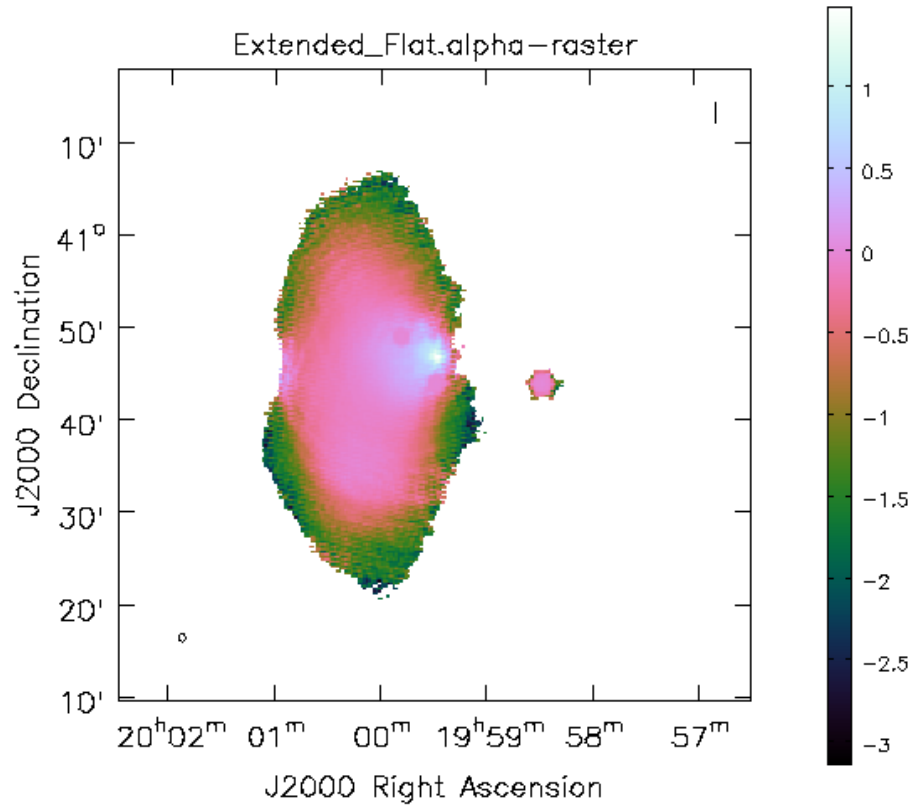


Figure 10: The pixel-wise spectral map of the flat-spectrum sky

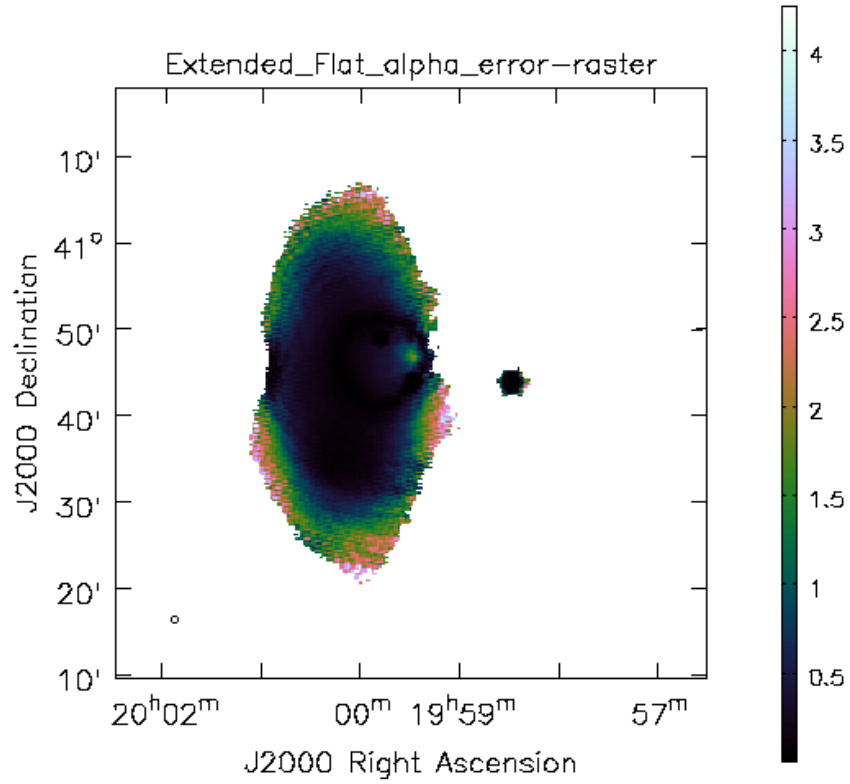


Figure 11: Map showing error on the spectrum estimate for Flat-spectrum sky

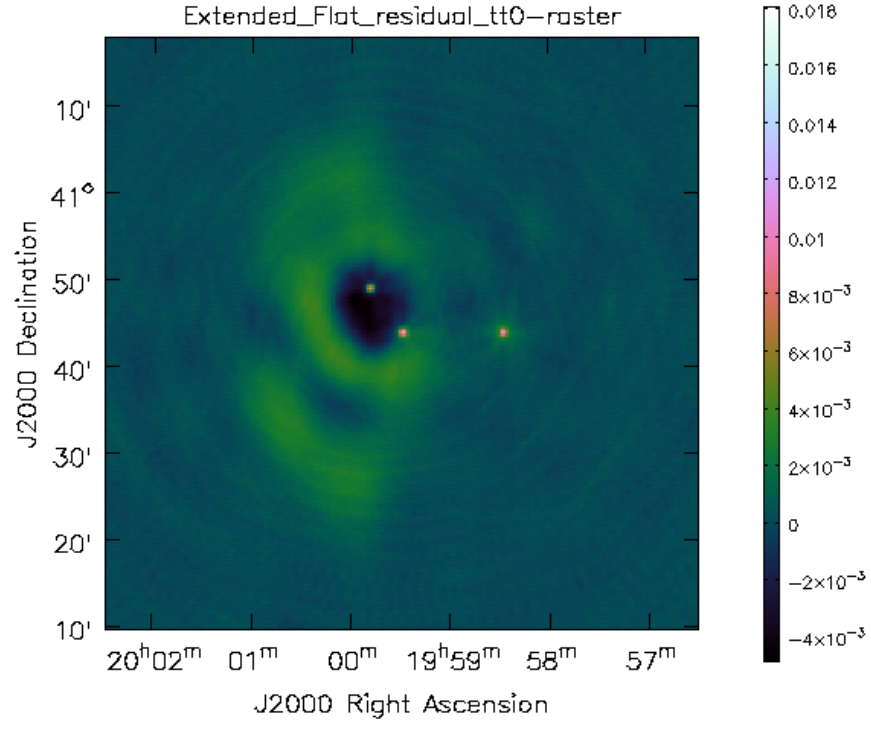


Figure 12: The zero-order residual image for Flat-spectrum sky

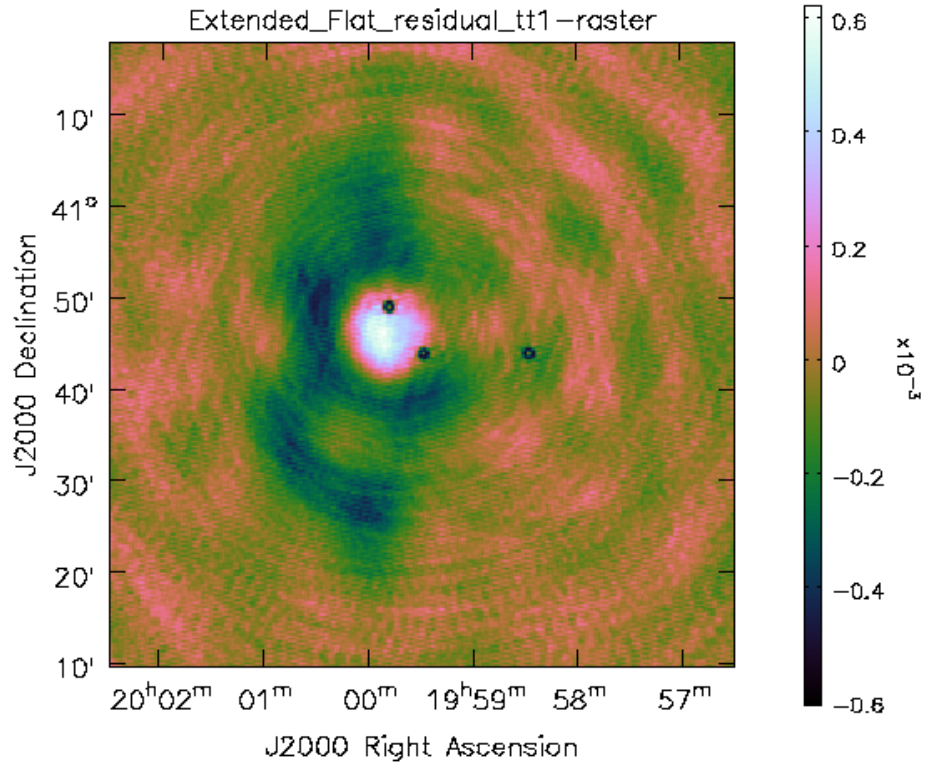


Figure 13: The first-order residual for the Flat-spectrum sky

3.2 A Steep-Spectrum Sky

Here, the reconstructed images from the Steep-spectrum sky are shown (true sky image shown in Figure 7-right panel)

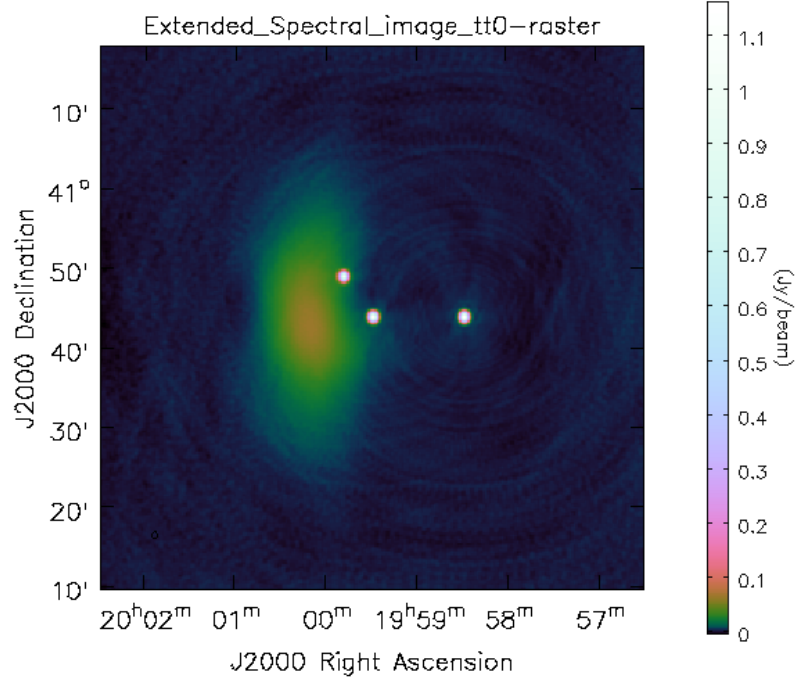


Figure 14: The zero-order image of the steep-spectrum sky

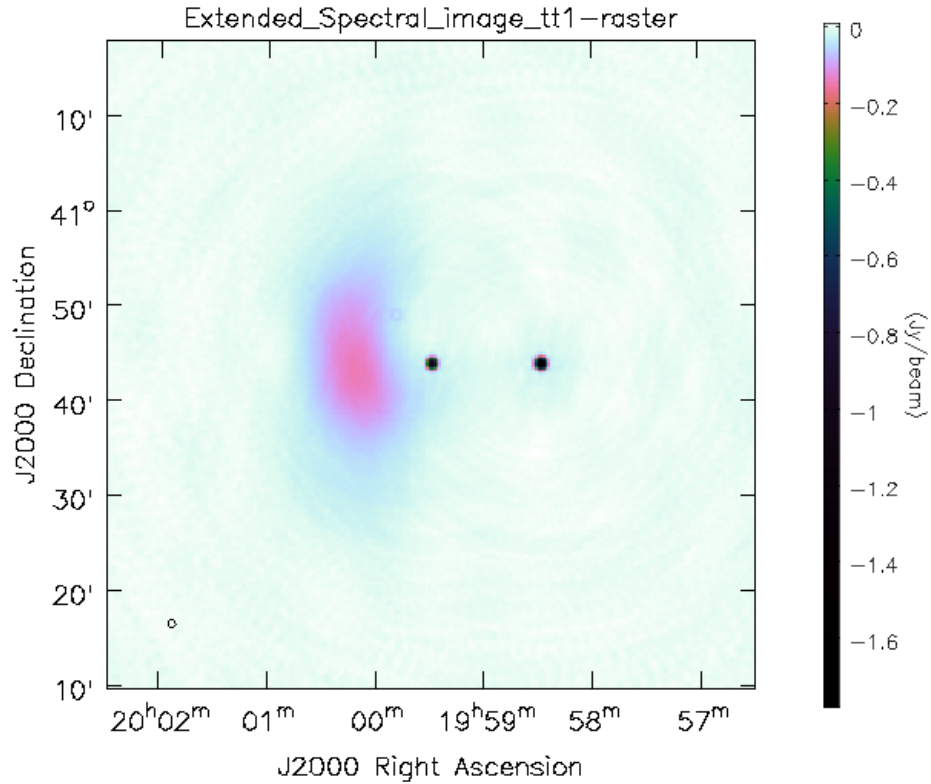


Figure 15: The first-order image of the steep-spectrum sky

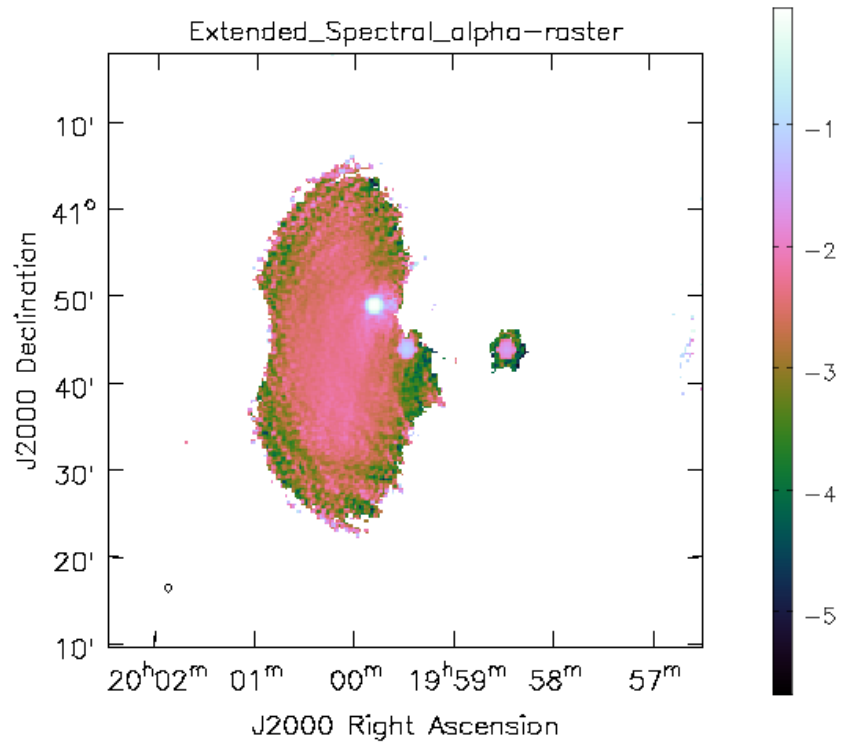


Figure 16: The pixel-wise spectral map of the steep-spectrum sky

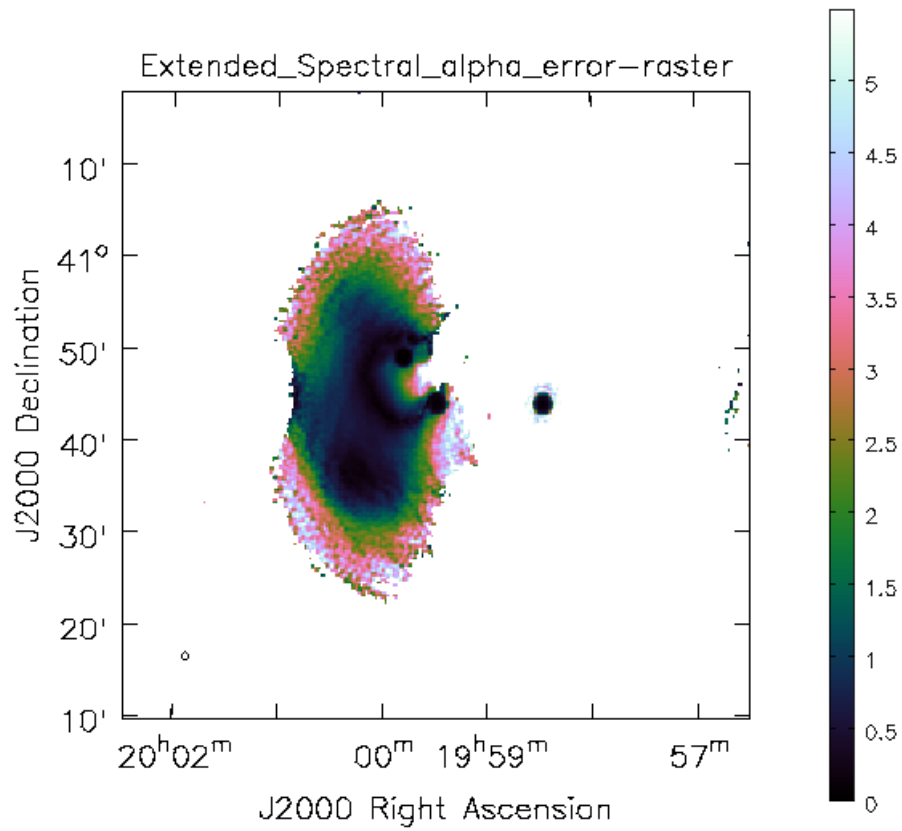


Figure 17: Map showing error on the spectrum estimate for Steep-spectrum sky

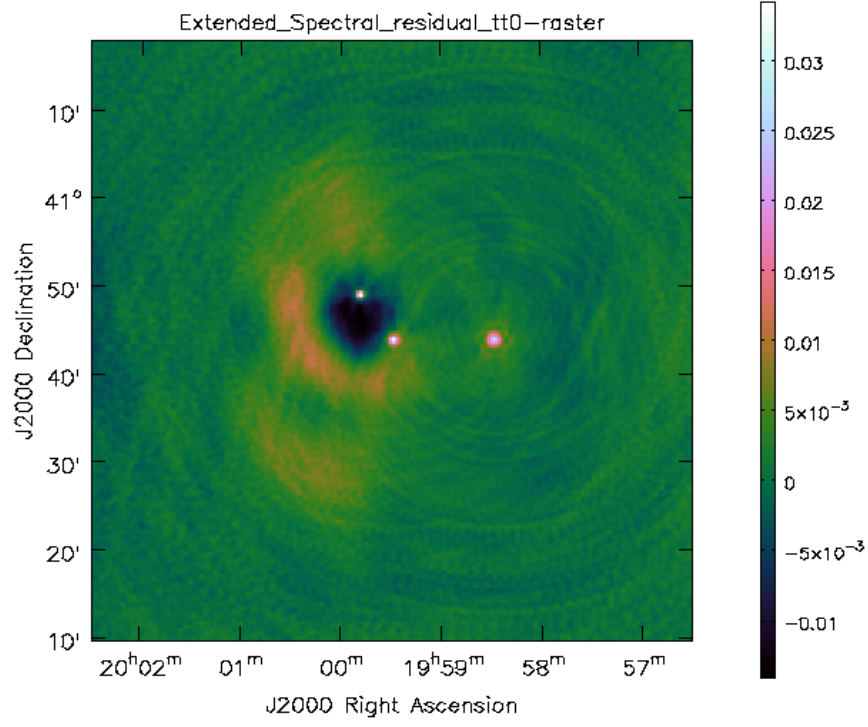


Figure 18: The zero-order residual image of the steep-spectrum sky

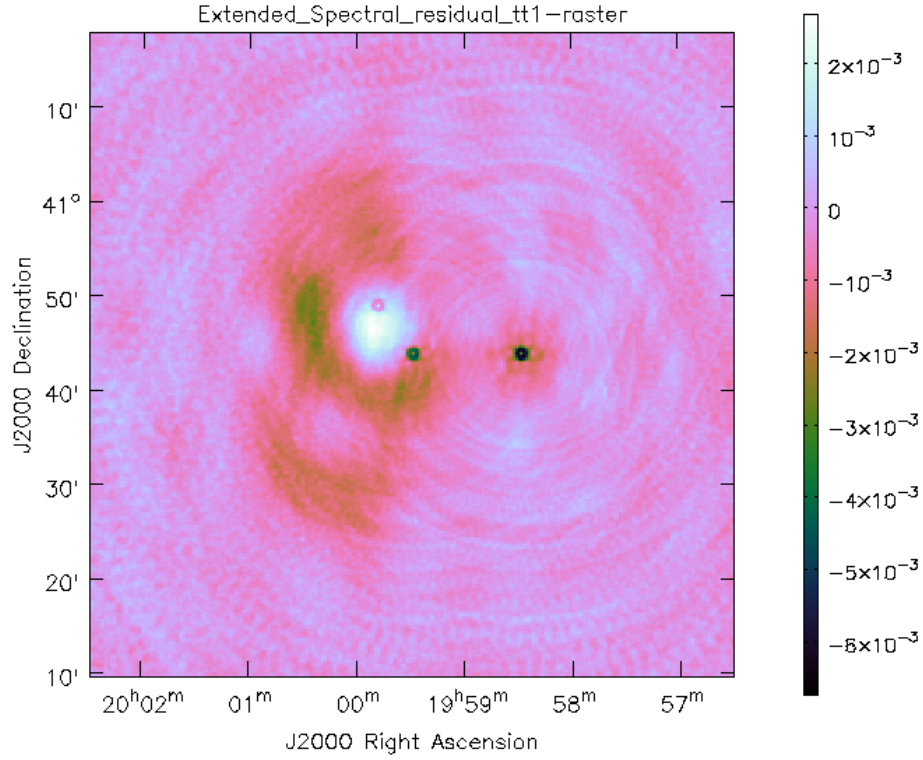


Figure 19: The first-order residual image for a steep-spectrum sky

3.3 Comments and Discussion on the Results

From the figures presented in the preceding section, it is seen that the algorithm works well for the given data set.

1. The algorithm for estimating the pixel-by-pixel spectral maps (figures 9 and 15) work well only at the centre of the extended cloud. This is because the spectrum in each pixel is the ratio of the terms \mathbf{I}_0 and \mathbf{I}_1 (Equation 5). Behaviour of these functions around the edges can be unpredictable, causing the estimate to go wrong.
2. The deconvolver has to run only within a narrow range with respect to the number of iterations, else there will either be insufficient convergence (if the number of iterations is too small) or artifacts in the spectral map (if the number of iterations is too large).
3. The single dish gain (pre-scaling) parameter also determines the performance of the algorithm, outside of a range of values. If the value is given to be too small, it can actually suppress the interferometer (u, v) data near the $(0, 0)$ region and cause the feathered data to become nearly zero in value. If its value is too large ($> \sim 15$), it will wash out the interferometer data and make the PSF too broad for a proper deconvolution to occur.

4 Summary of the Project

The project aimed to achieve the following goals :

1. Solve the short-spacing problem encountered by interferometers.
2. To combine the wideband multi-frequency data from a single-dish radio telescope and interferometer.
3. To evaluate the efficacy of a joint-deconvolution algorithm where the single-dish data was inserted into the interferometer data *before* the creation of an image, as compared to the traditional approach of a *post-facto* combination.
4. To estimate the spectrum of extended sources by creating a wideband image.
5. To prototype and test the working of an algorithm in order to accomplish these tasks.
6. To try this algorithm on real data from an actual astronomical observation.

All the objectives except the last one were achieved in the project. The last one can be achieved through a fairly simple extension of this work, which will be tried as and when the data from both these telescopes becomes available.

5 Knowledge and Skills gained during this Project

5.1 New concepts learned during the project

- **Radio Interferometry** : In-depth knowledge of the technique and mathematics of radio interferometry, including but not limited to computational implementation of 2-D Fourier transforms, Van Cittert-Zernicke theorem, (u, v) sampling, synthesis imaging with radio interferometer telescopes.
- **Radio Imaging** : Process of creation of an image from interferometer and single-dish data, role of deconvolution in synthesis imaging, multi-frequency synthesis imaging, imaging algorithms - Hogböm CLEAN and MTMFS.
- **Image Processing** : Concept of a pixel, image cell size, notion of linear time-invariant and linear shift-invariant systems, 2-D Fourier transforms, idea behind use of a specific kernel for detecting specific features in an image, image gridding, image weighting and its impact on the final synthesised image, combination of two images in the Fourier domain by means of a weighted average.
- **Algorithms and Data structures** : Their role in signal/image processing, implementation of convolution and deconvolution in well-known libraries like python's `scipy` and `numpy`, image representation as a 2-D array data structure and its manipulation in both the image domain and the Fourier domain, understanding the basic theory of the Fast-Fourier-Transform (FFT) algorithm.
- **Optimisation and Least-Squares minimisation** : Understanding the condition for applicability of the least-squares optimisation method, deriving the matrix conditions for calculating the coefficients.

5.2 Programming skills gained during this project

- **Programming with python** : In-depth understanding and application of toolboxes in python's `scipy` and `numpy` modules, programming in the `CASA` and `ipython` interactive IDE environment.
- **Numerical analysis and computation with python** : Fourier Transforms, convolution (both in the spatial domain and Fourier-transformed space), Calculation of autocorrelation function and estimating the power spectrum from it *via* the Weiner-Khinchin theorem, simulation of a simple antenna pattern and using it to create a simulated image, optimisation and least-squares minimisation - implement and demonstrate a program to fit a polynomial to a bunch of noisy data points using python's `linalg` library and comparing it with the standard tool package available in `numpy` and evaluating which is better.
- **Data Structures with python** : Handling of images in python, image cubes as a stack of multiple arrays, python's `copy` module, shallow copies and deep copies in python, different kinds of variable bindings in python (bind-to-variable name *vs.* creating a separate data structure), handling of python's `dictionary` data type, creating a new data structure using python.
- **Graphics and plotting with python** : Use of `matplotlib` plotting package from python, plotting of 1-D, 2-D and 3-D plots using this package, interactive plotting with `matplotlib`'s `ion()` command, plotting images and intensity maps.
- **Familiarisation of the CASA program**: use of `CASA`'s `tclean()` task, image plotting with `CASA` and understanding how it implements imaging and deconvolution algorithms.

5.3 Practical Field Training

- **Training** : Visiting the site of the Very Large Array (VLA) radio telescope, understanding the functioning of the antennas and the associated hardware as well as software backends that go with it.
- **Public Outreach Programmes** : Give two guided tours of the VLA to the public on its open day, explaining all the salient features of the facility.

6 Acknowledgements

This project was conducted under the National Radio Astronomy's Summer Student Research Assistantship programme, under the guidance of Dr. Urvashi Rau Venkata. This project also fulfills the compulsory summer training/internship requirements, mandated as part of the B. Tech (Hons.) course in Instrumentation Engineering, under the Dept. of Electrical Engineering, Indian Institute of Technology Kharagpur.

Many thanks to Sanjay Bhatnagar and Kumar Golap for their help in resolving several technical issues. The author wishes to acknowledge the great amount of help provided by Amy Mioduszewski in her role as the Coordinator of the Summer Student Program at the NRAO. The National Radio Astronomy Observatory is a facility of the National Science Foundation operated under cooperative agreement by Associated Universities, Inc.

7 References and Bibliography

1. Wikipedia webpage on radio telescopes : https://en.wikipedia.org/wiki/Radio_telescope
2. "Low Frequency Radio Astronomy", *ed.* Jayaram N. Chengalur, Yashwant Gupta and K.S. Dwarakanath, National Centre for Radio Astrophysics, May 2003.
3. "Interferometry and Synthesis in Radio Astronomy", Thompson *et. al*, 3rd ed., Springer International Publishing, June 2016.
4. Wikipedia webpage on interferometry : <https://en.wikipedia.org/wiki/Interferometry>
5. "Statistical Optics", by M. Born and E. Wolf, Dover Publications, 1959.
6. NRAO's CASAguides webpage on feathering : <https://casa.nrao.edu/Release3.4.0/docs/userman/UserManse30.html>

7. "A multi-scale multi-frequency deconvolution algorithm for synthesis imaging in radio interferometry", U. Rau and T. J. Cornwell, *Astronomy and Astrophysics* 532, A71 (June 2011).
8. "Parameterized Deconvolution For Wide-Band Radio Synthesis Imaging", Urvashi Rau Venkata, Ph.D Thesis, New Mexico Institute of Mining and Technology (2011)
9. CASA guide on the MTMFS deconvolver and `tclean()` task :
https://casaguides.nrao.edu/index.php/TCLEAN_and_ALMA
10. Talk on Wideband Imaging and Deconvolution :
<https://science.nrao.edu/science/meetings/2014/14th-synthesis-imaging-workshop/lectures-files/SIW2014.WidebandImaging-UR.pdf>

8 Appendix

8.1 Further extension of this work

This work dealt with combination of data from both the interferometer as well as the single-dish instrument. As an important spin-off, the code can be modified to do the whole procedure for either the pure single-dish image or the pure interferometer image for handling cube images (multiterm imaging algorithms exist for pure interferometers). As a brief example of this, the plots (the two images, spectrum and spectral error) from the single dish-only data is presented below :

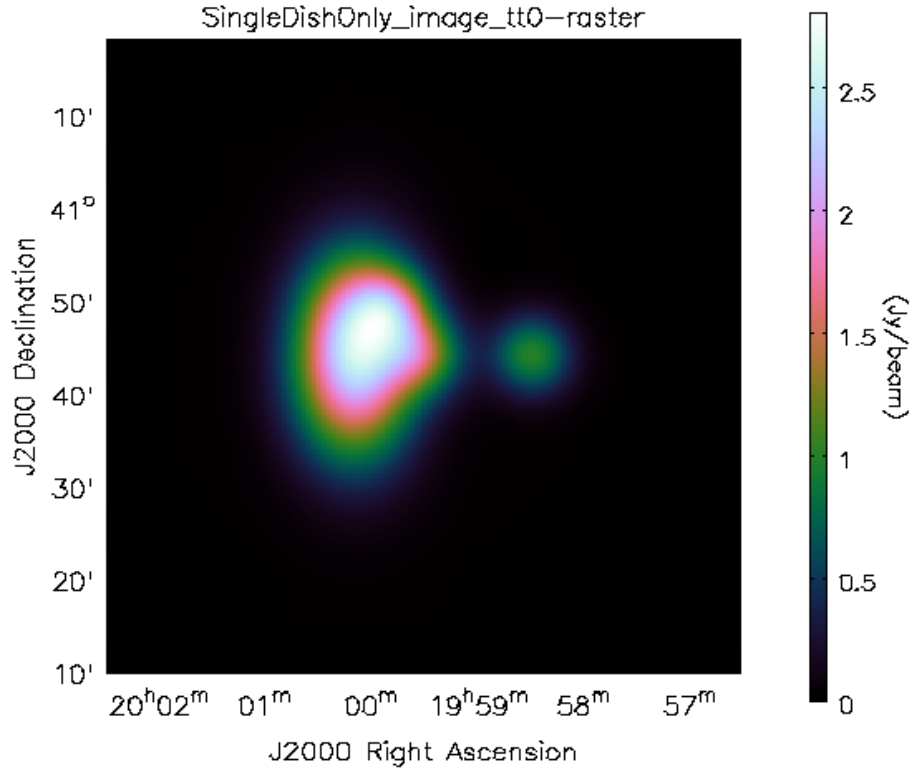


Figure 20: The zero-order image of the sky using only the single-dish data in the Wideband Joint deconvolution algorithm

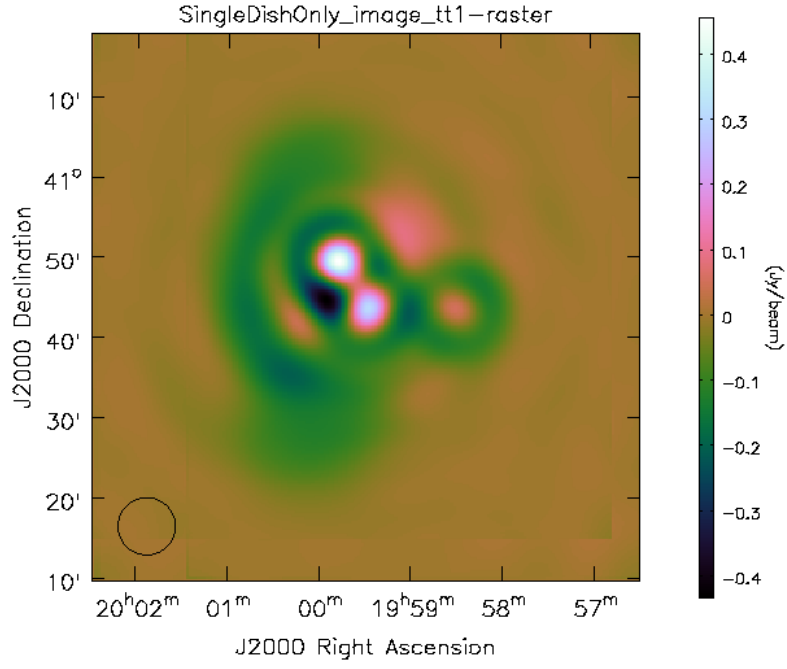


Figure 21: The first-order image of the sky using only the single-dish data in the Wideband Joint deconvolution algorithm

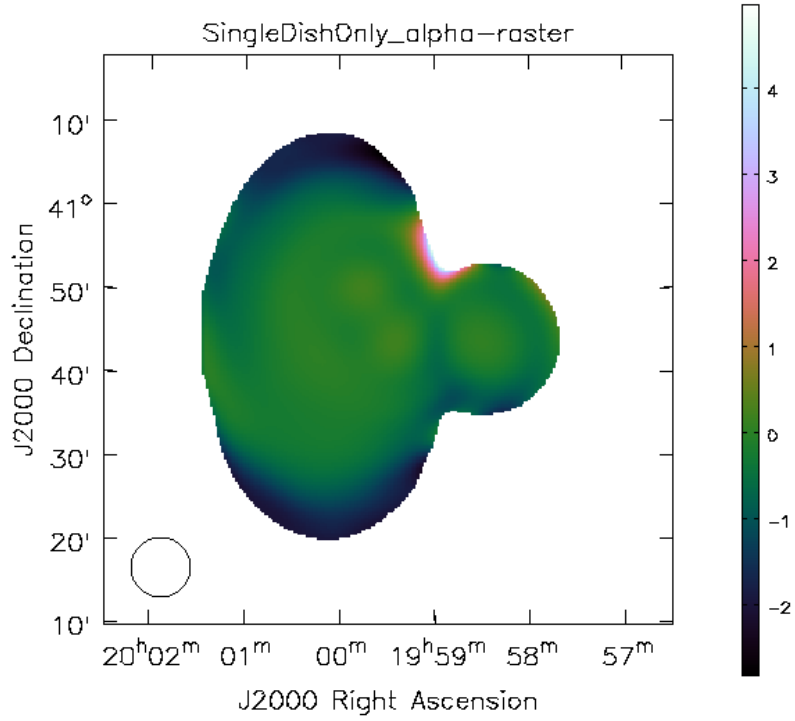


Figure 22: Pixel-wise spectrum map estimated by the algorithm, using only single-dish data.

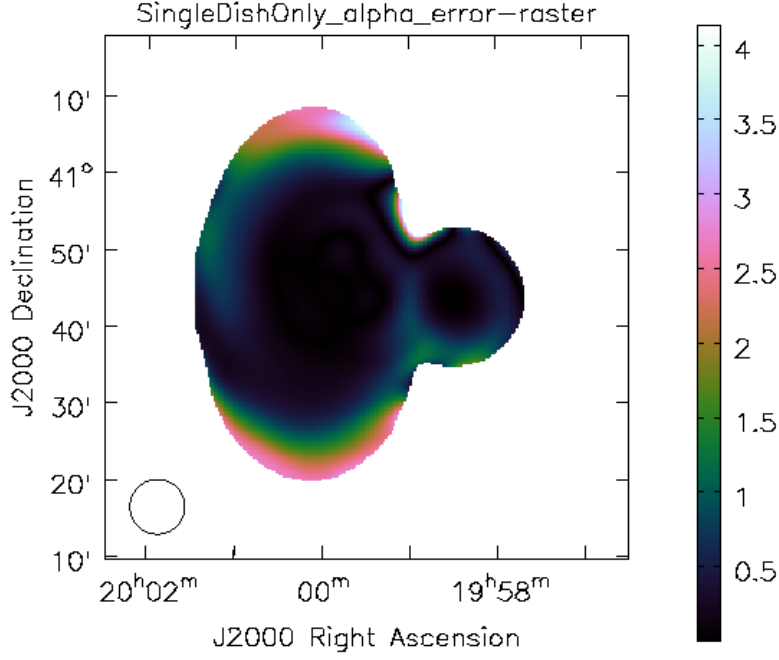


Figure 23: Pixel-wise map showing error in the spectrum estimate using only single-dish data

As can be seen, this code works very well for the pure single-dish data as well for the combination in terms of estimating the spectrum. As expected, the resolution on the objects seen in the plot is very coarse as compared to the case where the interferometer visibilities were also present. This combination algorithm will prove useful to the ALMA⁸ and possibly the Square Kilometer Array (SKA) radio telescope which will come up in the near future.

8.2 Location of the Source Code and Data Use

The source code of this entire project (along with a few sample data sets) is open for viewing can be accessed online, upon request to either of the two persons : (The whole project will be released online at a future date)

- Dr. Urvashi Rau Venkata, Associate Scientist, CS, National Radio Astronomy Observatory, 1003 Lopezville Rd., Socorro, New Mexico 87801.
email : rurvashi@aoc.nrao.edu
- Nikhil Vijay Naik, 4th year undergraduate student, Department of Electrical Engineering, Indian Institute of Technology, Kharagpur, West Bengal, India - 721302.
email : nikhilnaik@iitkgp.ac.in

⁸The Atacama Large Millimeter Array